SCIENTIFIC REPORTS

OPEN

SUBJECT AREAS:
MECHANISMS OF DISEASE
ION CHANNELS IN THE NERVOUS SYSTEM
POTASSIUM CHANNELS
EXPERIMENTAL MODELS OF DISEASE

Received
18 March 2013

Accepted
26 July 2013

Published
15 August 2013

Correspondence and requests for materials should be addressed to J.E.A.B. (braunj@ucalgary.ca)

* These authors contributed equally to this work.

The Large Conductance, Calcium-activated K^+ (BK) Channel is regulated by Cysteine String Protein

Barry D. Kyle[2]*, Eva Ahrendt[1]*, Andrew P. Braun[2] & Janice E. A. Braun[1]

[1]Department of Physiology and Pharmacology, The Hotchkiss Brain Institute, Faculty of Medicine, University of Calgary, Calgary, Alberta, Canada T2N 4N1, [2]Department of Physiology and Pharmacology, The Libin Cardiovascular Institute, Faculty of Medicine, University of Calgary, Calgary, Alberta, Canada T2N 4N1.

Large-conductance, calcium-activated-K^+ (BK) channels are widely distributed throughout the nervous system, where they regulate action potential duration and firing frequency, along with presynaptic neurotransmitter release. Our recent efforts to identify chaperones that target neuronal ion channels have revealed cysteine string protein (CSPα) as a key regulator of BK channel expression and current density. CSPα is a vesicle-associated protein and mutations in CSPα cause the hereditary neurodegenerative disorder, adult-onset autosomal dominant neuronal ceroid lipofuscinosis (ANCL). CSPα null mice show 2.5 fold higher BK channel expression compared to wild type mice, which is not seen with other neuronal channels (i.e. $Ca_v2.2$, $K_v1.1$ and $K_v1.2$). Furthermore, mutations in either CSPα's J domain or cysteine string region markedly increase BK expression and current amplitude. We conclude that CSPα acts to regulate BK channel expression, and consequently CSPα-associated changes in BK activity may contribute to the pathogenesis of neurodegenerative disorders, such as ANCL.

Large conductance, calcium-activated K^+ channels (BK channels) are widely distributed throughout the CNS, and play an important role in regulating neuronal action potential duration, the extent of fast after-hyperpolarization and burst firing frequency[1–3]. BK channels are also prominent in the pre-synaptic membrane, where they regulate the magnitude and timing of depolarization-evoked calcium influx, thereby influencing neurotransmitter release at the synapse[4–8]. Genetic deletion of BK channel subunits in mice[9,10] and a gain-of-function channel mutation in humans[11,12] are associated with neurological disorders, such as ataxia and epilepsy. It is thus evident that alterations in neuronal BK channel activity give rise to CNS dysfunction and for this reason, it is critical to understand the mechanisms underlying BK channel regulation. In this study, we provide evidence that the co-chaperone, cysteine string protein (CSPα), controls the cell surface density of neuronal BK channels.

CSPα is a synaptic vesicle-associated protein that is broadly expressed in the nervous system and displays unique anti-neurodegenerative properties[13,14]. It is a member of the large J protein family[15]. CSPα contains an N terminal J domain and a middle region displaying a string of 13–15 cysteine residues[16], which are subject to palmitoylation and critical for anchoring CSPα to synaptic vesicles[17,18]. CSPα is active as a trimeric complex, composed of the heat shock cognate protein of 70 kDa (Hsc70) and the small tetratricopeptide protein (SGT)[19–21].

While not essential for neurotransmitter release, CSPα is required to maintain synaptic function in mice after 3 weeks of age. Genetically-modified mice lacking CSPα appear normal at birth, but around postnatal day 20, they develop progressive motor deficits and CNS degeneration, followed by early lethality between days 40–80[14]. The synapse loss in CSPα null mice is activity-dependent and synapses that fire frequently, such as those associated with photoreceptors and GABAergic neurons, are lost first[22,23]. It has been reported that 22 proteins are decreased in CNS synapses from CSPα knockout mice[24] and several other synaptic proteins appear to be putative clients for the CSPα chaperone system, based on association studies[25–28]. Which client protein(s) is critical for triggering the cascade of events leading to degeneration and which changes are downstream of the primary event is a current biological question. Specifically, studies in CSPα null mice reveal that the t-SNARE SNAP25 (synaptosomal associated protein of 25 kDa), which is fundamental for exocytosis, and the GTPase dynamin1, essential for endocytosis, are clients of the CSPα chaperone complex, leading to the prediction that loss of CSPα function would impair vesicle trafficking in neurons[24,29–32]. Interestingly, degeneration in CSPα null mice can be rescued by over-expression of wild-type, but not inactive mutants of SNAP-25[30]. Moreover, over-expression of α-synuclein, which does not have homology to either CSPα or SNAP-25, prevents degeneration in CSPα-null mice[29]. Exactly

how these proteins compensate for loss of CSPα is not currently known. The importance of CSPα in synapse protection is well established, but our knowledge of the mechanistic events underlying this protection is weak and many questions remain.

The activity of BK channels is subject to an elaborate array of regulatory mechanisms including; modulatory accessory subunits[33], phosphorylation[34], palmitoylation[35] and alternative splicing[36]. In this study, we demonstrate that CSPα regulates cell surface expression of BK channels, which would be expected to modify synaptic function. We report that neuronal BK channel expression is increased in the brain tissue of CSPα null mice. We additionally demonstrate that mutation of a highly conserved motif in the J domain (i.e. HPD to AAA substitution) and deletion of residue 116 or replacement of Leu115 by Arg in the cysteine string region of CSPα increases BK current by selectively increasing cell surface BK channel expression. These data reveal a novel chaperone-based cellular mechanism that regulates BK channel expression in the CNS. These observations raise the intriguing possibility that CSPα-related dysregulation of BK current density may alter neuronal excitability and contribute to the pathogenic sequence of events in one or more neurodegenerative disorders.

Results

BK channel was identified as a possible target protein of the CSPα chaperone complex based on our initial observation of robust changes in BK channel density in neuroblastoma cells co-expressing CSPα mutant proteins. Members of the J-protein family have been reported to regulate the trafficking/expression of several ion channel types, including: the hERG (human ether-a-go-go related gene) K^+ channel[37,38], CFTR (cystic fibrosis transmembrane conductance regulator)[39] and the K_{ATP} channel (ATP-sensitive K^+ channel)[40], leading to the prospect that J-proteins are components of the cellular machinery that make 'triage' decisions regarding whether ion channels are trafficked and/or retained at the cell surface or degraded. To study the relationship between CSPα and BK channel expression, we first measured BK channel expression in wild-type and CSPα knockout mice. CSPα null mice are normal at birth, but after a lag period of 2–3 weeks, they stop gaining weight, and develop blindness, activity-dependent neuronal degeneration and progressive motor impairments. CSPα null mice typically die prematurely between 40–80 days[14]. Heterozygous mutant mice contain less CSPα protein than wild-type controls, while homozygous mutant mice lack detectable CSPα[14]. Figure 1 shows the expression of BK channel, $Ca_v2.2$, Kv1.1

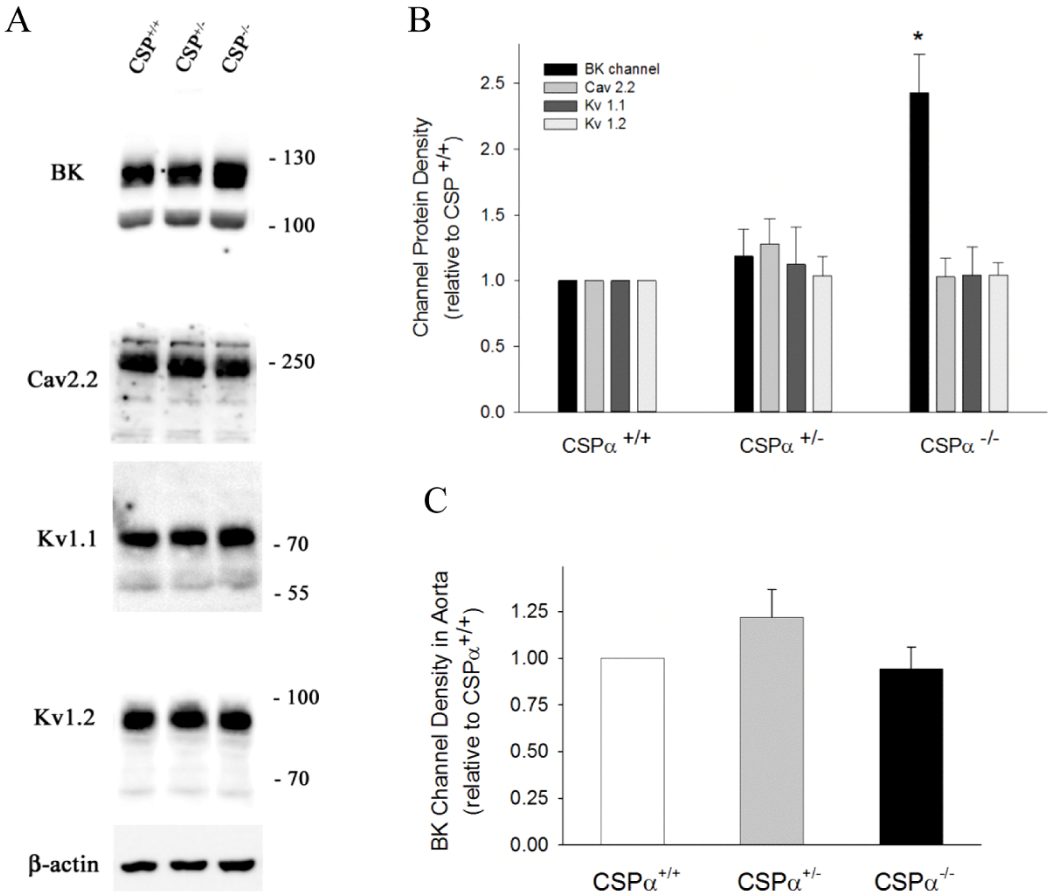

Figure 1 | Comparison of protein levels for BK, $Ca_v2.2$, $K_v1.1$ and $K_v1.2$ channels in whole brain tissue from CSPα wild-type, heterozygous and null mice. (A) Representative western blot data of the pore-forming α subunits of BK channel, $Ca_v2.2$ channel, $K_v1.1$ and $K_v1.2$ channels detected in synaptosome-enriched membrane fractions prepared from whole brain (age P23–27). The total protein loaded per lane was 40 μg; detection of β-actin on the same blots was used to verify equal loading amongst the various lanes. The data shown in panel A were selected from full-length western blot images, which are displayed in Supplementary Figure 1. (B) Histogram showing average data for BK, $Ca_v2.2$, $K_v1.1$ and $K_v1.2$ channel protein in the wild-type, heterozygous and null brain samples quantified by camera-based detection of emitted chemiluminescence. To perform quantification, the ratio of detected channel protein to β-actin for a given sample was calculated for all three genetic backgrounds. Channel density data for the heterozygote and null tissues were then normalized to the wild-type tissue by dividing all calculated ratios by the wild-type ratio for a given channel species. (C) Histogram showing BK channel expression detected in aorta from CSPα heterozygous and null mice relative to wild-type mice. Quantification of BKα subunit detection was performed as described in panel B. Averaged Western blot data were derived from 5–6 animals (panel B) and 3–4 animals (panel C) of each genetic background (2–3 litters). * indicates a statistically significant difference from the heterozygote and wild-type values, as determined by one-way ANOVA and a Tukey's post-hoc test; $p < 0.05$.

and $K_v1.2$ channels in whole brain synaptosomal membrane fractions from CSP$\alpha^{-/-}$, CSP$\alpha^{-/+}$, and CSP$\alpha^{+/+}$ mice, as assessed by western blotting. BK channel expression is significantly elevated in CSPα null mice, whereas heterozygotes show expression levels similar to the wild-types. Moreover, the observed increase in BK channel is selective, as the tissue levels of $Ca_v2.2$, $K_v1.1$ and $K_v1.2$ channels are not significantly altered in the brains of either the CSP$\alpha^{-/-}$ or CSP$\alpha^{-/+}$ mice compared with the wild-type control. Interestingly, BK channel α subunit mRNA was not elevated in the brains of CSP$\alpha^{-/-}$ mice, as determined by quantitative RT-PCR (Table 1), suggesting that the increased level of BK channel protein in CSP$\alpha^{-/-}$ brain tissue is not due to a transcriptional event. It is also well known that CSPα is primarily expressed in tissues exhibiting regulated secretion, such as the brain and pancreas[16,41]. In murine aortic smooth muscle, which has prominent BK channel levels, we observed no difference in the average level of BKα subunit expression amongst the three genetic backgrounds (Figure 1C). Given that CSPα is not expressed in the aorta, this finding is not unexpected.

In order to gain mechanistic insight into the influence of CSPα on BK channel proteostasis, we generated a murine CNS-derived catecholaminergic (CAD) cell line[42] stably expressing a murine neuronal BK channel ([43]; see Methods Section) that would enable rigorous electrophysiological and immunocytochemical analyses of BK channel levels. The expression of BK channels in these cells was measured in the presence of myc-tagged CSPα or the myc-tagged loss-of-function mutant $CSP\alpha_{HPD\text{-}AAA}$. Functionally, mutation of the HPD motif (residues 43-45) in CSPα disrupts the integrity of the highly conserved J domain, thereby preventing CSPα from activating Hsp70/Hsc70 to carry out conformational protein folding[44]. Expression of the loss-of-function mutant $CSP\alpha_{HPD\text{-}AAA}$ is thus expected to override the activity of endogenous CSPα in CAD cells and act in a dominant-negative fashion[45]. Figures 2A and B show Western blot analysis and corresponding mean data of BK channel expression in the stable CAD cell line 48 h following transient transfection with myc-tagged CSPα, $CSP\alpha_{HPD\text{-}AAA}$ or pCMV plasmid (negative control). As expected, 3 distinct species of CSPα were identified by Western blot in transfected cells; the 26 kDa immature form, the 34 kDa mature palmitoylated protein and the 70 kDa CSPα dimer[42,46]. In the presence of $CSP\alpha_{HPD\text{-}AAA}$, BK channel expression was elevated ~6-fold (657.5 ± 175.4%) compared with the plasmid control (100%). In contrast, increased levels of wild-type CSPα did not significantly change BK channel expression. As genetic knockout of CSPα is associated with elevated BK channel protein in brain tissue (Figure 1), we speculated that CSPα may interact either directly or indirectly with neuronal BK channels under native conditions. However, we were unable to capture stable CSPα-BK channel complexes from wild-type mouse brain using a classic immunoprecipation strategy (n = 4, data not shown). Such an observation may either reflect a lack of complex formation between native CSPα and BK channels, or that such putative interactions are of a transient, low affinity nature and not detectable using this analytical approach.

As CSPα is a member of the highly conserved J protein family, we reasoned that other J proteins may also influence BK channel expression. Hsp40 (heat shock protein of 40 kDa) is a cytosolic member of the J protein family that is expressed constitutively, as well as in response to cell stress. Like CSPα, Hsp40 is neuroprotective and acts in concert with Hsc70, but the exact mechanism underlying its cell protective actions remains poorly characterized[47]. In CAD cells stably expressing BK channels, transient expression of either wild-type Hsp40 (99.3 ± 21.7%) or the loss-of-function mutant $Hsp40_{HPD\text{-}AAA}$ (94.7 ± 9.5%) did not alter BKα subunit expression (Figure 2B). Collectively, these results indicate that the loss-of-function mutant $CSP\alpha_{HPD\text{-}AAA}$ leads to a selective increase in BK channel levels, whereas an equivalent mutation in Hsp40, a related J protein, has no effect.

It has been reported that BKα subunits can undergo palmitoylation[35], prompting us to examine whether other palmitoylated proteins may also be increased in the presence of the CSPα mutant $CSP\alpha_{HPD\text{-}AAA}$. As shown in Figure 2C, $CSP\alpha_{HPD\text{-}AAA}$ did not increase expression of the palmitoylated proteins[48,49] SNAP25, syntaxin1, GAP43 (growth associated protein of 43 kDa), and flotillin in BK stable CAD cells. In synaptosomes from CSPα null mice, we also did not observe changes in the expression of $K_v1.1$ (Figure 1A), another protein reported to be palmitoylated[50].

In order to evaluate the influence of mutant forms of CSPα on cell surface expression of functional BK channels, we carried out whole cell patch clamp electrophysiology to quantify active BK channels in single CAD cells. To distinguish BK channel current from endogenous voltage-gated K^+ channels (i.e. K_v1-type channels), we utilized 4-aminopyridine (4-AP, 5 mM) to block these channels and measured the remaining whole cell currents in the absence and presence of the highly selective BK channel inhibitor, penitrem A (100 nM)[51]. Figure 3A shows a current-voltage plot of the penitrem A-sensitive whole cell current density recorded from CAD cells stably expressing BK channels that have been transiently transfected with either wild-type or mutant forms of CSPα. BK current density was significantly greater in the presence of the $CSP\alpha_{HPD\text{-}AAA}$ mutant compared with eGFP-expressing control cells, demonstrating higher surface

Table 1 | BK Channel (KCNMA1) mRNA levels in wild-type and CSPα knockout mice[a]

Animal	KCNMA1 C_q	ACTB C_q	ΔC_q	$\Delta\Delta C_q$	KCNMA1 expression relative to WT ($2^{-\Delta\Delta Cq}$)
Wild-type					
1	21.42 ± 0.20	18.84 ± 0.20	2.58 ± 0.12		
2	21.50 ± 0.37	18.86 ± 0.25	2.65 ± 0.30		
3	21.66 ± 0.16	19.05 ± 0.11	2.61 ± 0.27		
4	21.55 ± 0.20	18.87 ± 0.13	2.68 ± 0.16		
5	21.85 ± 0.27	18.60 ± 0.04	3.25 ± 0.24		
Average	21.60 ± 0.41	18.84 ± 0.43	2.75 ± 0.34	0.00 ± 0.68	1.0 (0.6 − 1.6)
CSPα $^{(-/-)}$					
6	22.05 ± 0.27	19.90 ± 0.17	2.15 ± 0.10		
7	22.03 ± 0.13	19.44 ± 0.10	2.59 ± 0.04		
8	21.66 ± 0.16	18.69 ± 0.09	2.97 ± 0.08		
9	21.25 ± 0.20	18.57 ± 0.13	2.68 ± 0.14		
10	21.58 ± 1.03	18.89 ± 1.00	2.69 ± 0.13		
11	21.65 ± 0.51	19.21 ± 0.53	2.60 ± 0.29		
Average	21.71 ± 0.55	19.12 ± 0.64	2.61 ± 0.27	−0.14 ± 0.61	1.1 (0.7 − 1.7)

BK channel (KCNMA1) mRNA levels were measured by qRT-PCR in whole brain tissue from both WT and CSPα null mice at post-natal age 23–27 days. mRNA levels were normalized to those of actin (ACTB). [a]Quantification cycle (C_q) values are expressed as the average determinations ± standard deviation from 3 to 4 separate analyses of each brain tissue. ΔCq values were determined and then averaged.

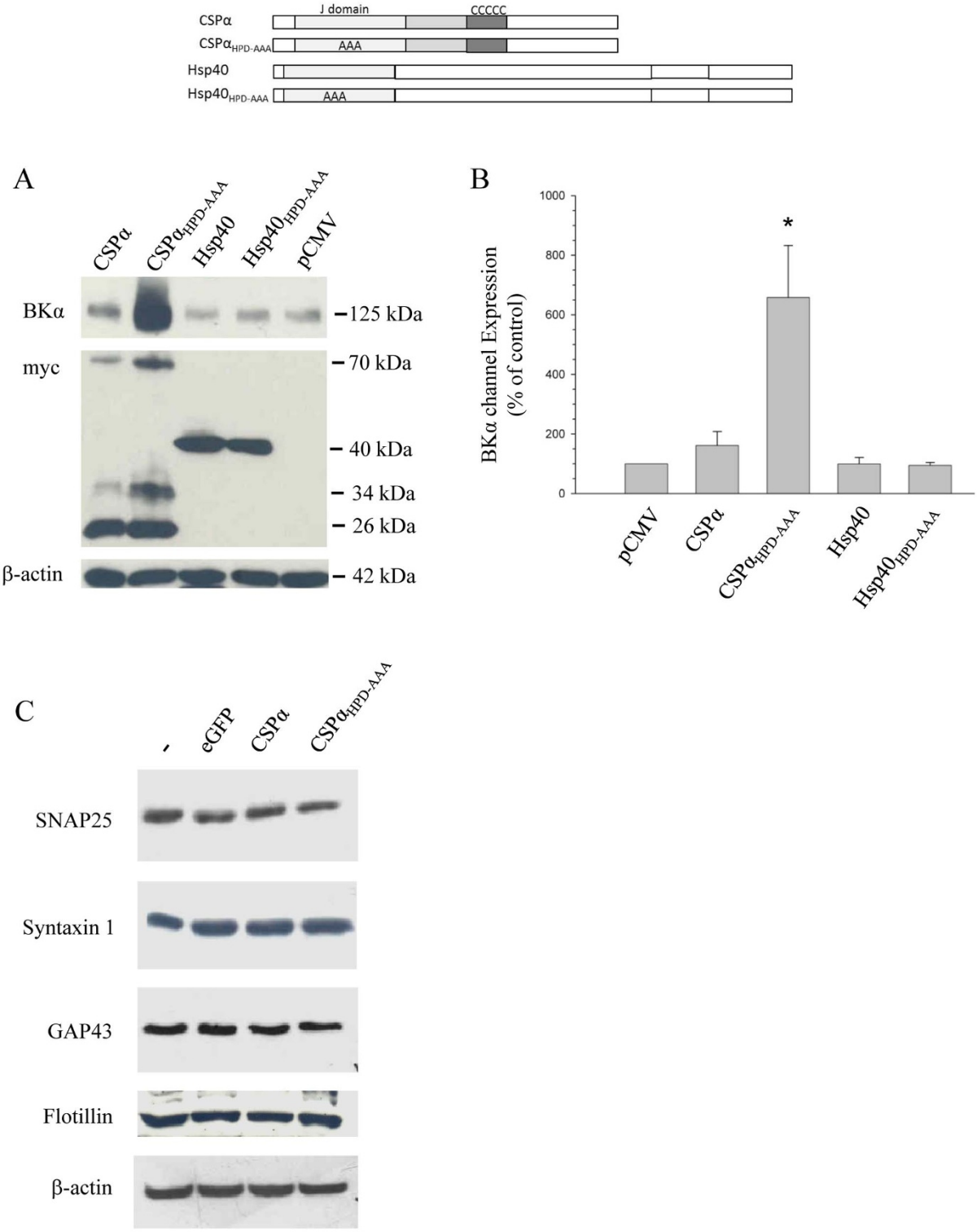

Figure 2 | CSPα$_{HPD-AAA}$ increases BK channel levels in stably-transfected, BK channel expressing CAD cells. A schematic of wild-type CSPα, CSPα$_{HPD-AAA}$, wild-type Hsp40 and Hsp40$_{HPD-AAA}$ is shown at the top of the Figure, in which the J domain and the cysteine string regions are indicated. (A) Western blot analysis of BKα subunit expression in BK stable, CAD cells transiently transfected with either myc-tagged CSPα or CSPα$_{HPD-AAA}$ (0.75 μg cDNA each), or 1 μg cDNA encoding either myc-tagged Hsp40 or Hsp40$_{HPD-AAA}$. pCMV plasmid (1 μg cDNA) was used as a transfection control. 48 h post-transfection, transfected cells were harvested and 30 μg of cell lysate were separated by SDS-PAGE, and probed with either an anti-BKα subunit antibody (upper) or an anti-myc antibody (middle). Detection of endogenous β-actin (lower) was used to verify similar sample loading. The BKα subunit data shown in the upper image of this panel were selected from a full-length western blot, which is displayed in Supplementary Figure 2A. The histogram (panel B) quantifies the relative changes in cellular BKα subunit expression in the presence of WT and HPD-AAA mutant forms of CSPα and Hsp40. (Panel C) shows a series of representative western blots of proteins reported to undergo palmitoylation. Soluble lysates were prepared from BK stable CAD cells transiently transfected with either wild-type CSPα or the HPD-AAA mutant, as indicated at the top of the panel. eGFP was used as a transfection control. Samples in the left hand column (denoted by the minus sign) are lysates from non-transfected cells. Detection of β-actin was used as a loading control. Results are representative of 4 independent experiments that all provided qualitatively similar data. Statistically significant differences between values were determined by -ANOVA, * $p < 0.05$.

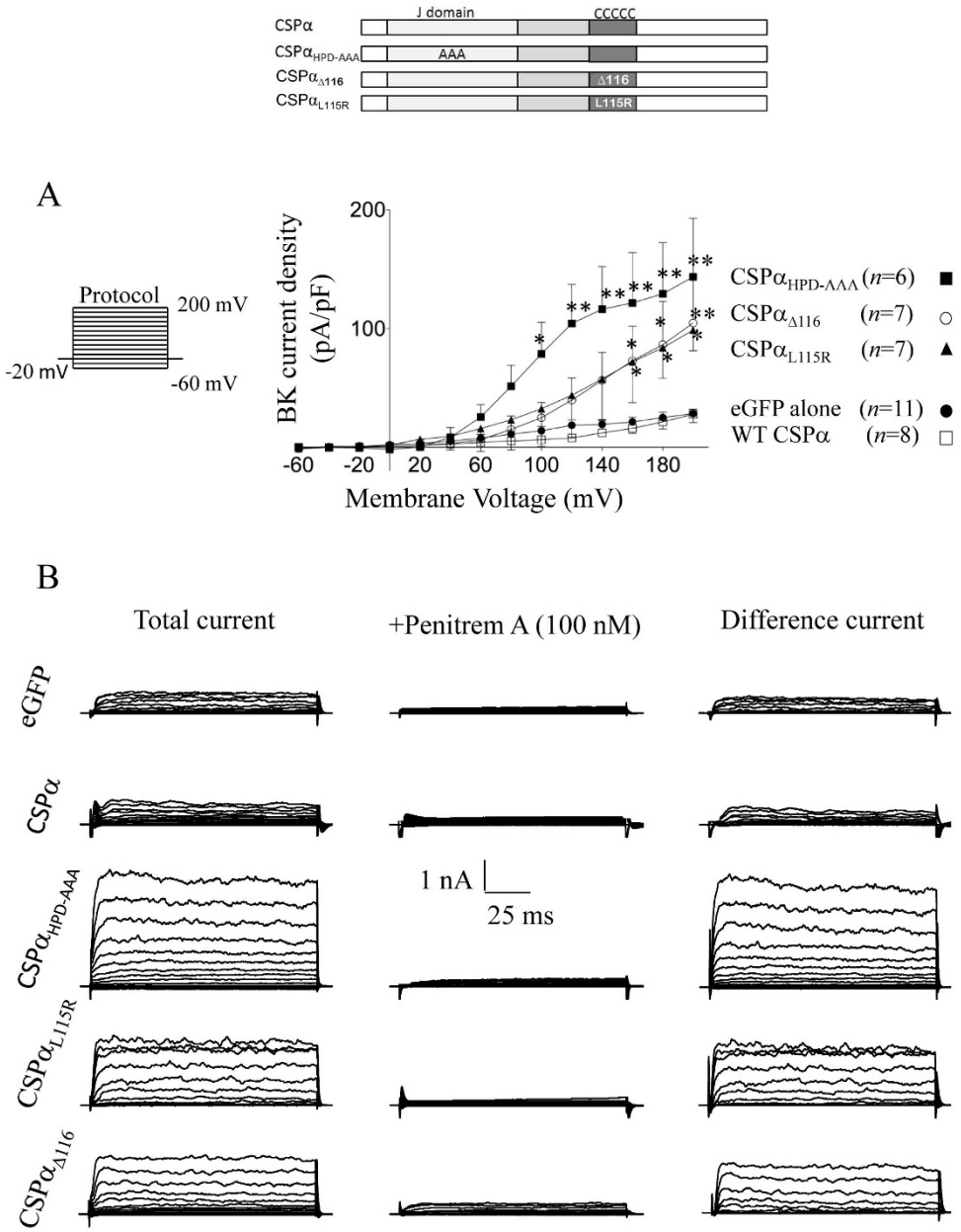

Figure 3 | CSPα$_{HPD-AAA}$ increases penitrem A-sensitive ionic current in BK channel stably-transfected CAD cells. Domain architecture of CSPα is shown at the top of the Figure. A. Electrophysiological analysis of BK stable CAD cells transiently transfected with either wild-type or mutant forms of CSPα. Single CAD cells were voltage clamped as depicted by the test pulse protocol shown on the left, and the selective BK channel inhibitor, penitrem A (100 nM) was used to isolate BK channel current. The current-voltage plot summarizes the penitrem A-sensitive, whole cell current density recorded from transfected cells, as described on the right hand side of the plot. Data are presented as mean ± SE, and statistically significant differences were determined using a one-way ANOVA and a Dunnett post-hoc test (vs. GFP alone); * ($p<0.05$), ** ($p<0.01$). B. Representative families of whole cell currents recorded from BK stable CAD cells transiently transfected with either wild-type or mutant forms of CSPα in response to voltages steps ranging from −20 to +200 mV. The left hand column displays total whole cell current recorded from cells under the indicated transfection conditions. The middle column shows current remaining in the presence of the BK channel blocker penitrem A, and the right hand column displays the calculated difference currents obtained by digitally subtracting the currents evoked in penitrem A from the total whole cell currents. Scale bars are indicated.

expression of functional BK channels. In contrast, transient expression of wild-type CSPα had no effect on single cell BK current density, which is consistent with western blot data demonstrating very little effect of exogenous wild-type CSPα on the level of BKα subunit protein in BK stable CAD cells (Figure 2B). Figure 3B shows representative families of membrane currents recorded from BK stable CAD cells in the absence and presence of penitrem A under the described transfection conditions. The right hand column displays the penitrem A-sensitive current obtained by digital subtraction (i.e. left hand column minus middle column). These data clearly demonstrate that the CSPα loss-of-function mutant HPD-AAA increases cell surface expression of functional BK channels.

The CSPα Palmitoylation Mutants CSP$_{116}$ and CSP$_{L115R}$ Increase BK Channel Expression. In 2011, it was reported that novel mutations in human CSPα (i.e. deletion of residue 116 or replacement of Leu115 by Arg) are directly linked to adult-onset autosomal dominant neuronal ceroid lipofuscinosis (ANCL)[52–54].

ANCL is a rapidly progressive, neurodegenerative disorder in young adults, characterized by psychiatric manifestations, seizures, progressive dementia and motor deficits. Detailed pathogenic mechanisms of these CSPα mutations have yet to be elucidated, but individuals afflicted with ANCL display phenotypes reminiscent of the progressive motor deficits observed in the CSPα KO mouse. Both these mutations interfere with the palmitoylation of CSPα's cysteine string region, which is important for anchoring CSPα to synaptic vesicles. To evaluate the cellular effects of these putative dominant negative mutations, we examined the impact of $CSP\alpha_{\Delta 116}$ and $CSP\alpha_{L115R}$ mutations on the level of functional BK channel in our CAD cells stably expressing neuronal BK channels. Analysis of BK channel activity in the presence of either $CSP\alpha_{\Delta 116}$ or $CSP\alpha_{L115R}$ is shown in Figure 3. BK channel current density is significantly greater in the presence of $CSP\alpha_{\Delta 116}$ and $CSP\alpha_{L115R}$ mutants compared with either wild-type CSPα or eGFP-expressing control cells, but the increases are less than that observed with the $CSP\alpha_{HPD\text{-}AAA}$ mutant. Collectively, these data indicate that CSPα dysfunction has a profound effect on BK channel expression in a KO mouse model, as well as a model neuronal cell line.

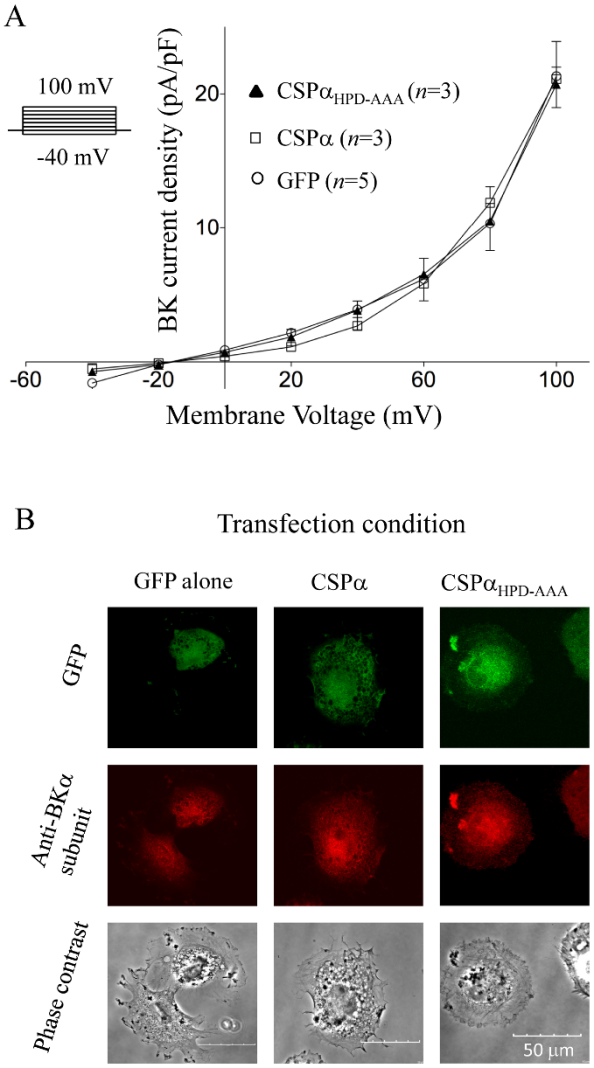

Figure 4 | Transient transfection with CSPα or $CSP\alpha_{HPD\text{-}AAA}$ has no effect on BK channels in A7r5 cells stably expressing murine brain BK channels. (A) Penitrem A-sensitive current density plot demonstrated no significant difference between the treatments at 100 mV. Evoked current was >5-fold higher than native A7r5 cell current at the same potential (data not shown). (B) Immunocytochemical staining of A7r5 cells with anti-BKα subunit antibody demonstrated BK channel expression. Data shown are representative of at least five different experiments.

To determine if the dysfunctional mutant $CSP\alpha_{HPD\text{-}AAA}$ could also affect BK channel activity in a non-neuronal cell, we recorded BK currents from a rat aortic smooth muscle cell line (i.e. A7r5[55]) stably transfected with the same BKα subunit cDNA used to create stable CAD cells. The data displayed in Figure 4 demonstrate that transient expression of either wild-type CSPα or $CSP\alpha_{HPD\text{-}AAA}$, as confirmed by immunocytochemistry (Figure 4B), had no effect on BK current density in A7r5 cells stably expressing BKα subunits. These findings are thus consistent with the observed lack of effect of CSPα knockout on native BK channel levels in mouse aorta (Figure 1C). Taken together, our data indicate that CSPα-mediated regulation of BK channels likely involves additional co-factors expressed in secretory cells, such as neurons.

Biochemical confirmation that the $CSP\alpha_{HPD\text{-}AAA}$-mediated increase in BK current density was associated with an increase in BK channel cell surface expression, along with the total cellular pool of channel protein, is shown in Figure 5. For this purpose, CAD cells stably expressing BK channels were first transfected with CSPα variants, followed by labeling of intact cells with biotin. Biotinylated cell surface proteins were then extracted from the total cell lysate by streptavidin pull-down, followed by western blot analysis. The degree of BK channel biotinylation was evaluated in the presence of transfected CSPα, $CSP\alpha_{HPD\text{-}AAA}$ or pCMV plasmid as a negative control. Consistent with the data displayed in Figures 2 and 3, the results shown in Figure 5A independently confirm that $CSP\alpha_{HPD\text{-}AAA}$ (lane 2) markedly increased the cell surface expression of BK channel compared with wild-type CSPα (lane 1) or the plasmid control (lane 3). These data are complemented by quantifiable changes in the immunofluorescence staining of BKα subunit expression in BK stable CAD cells that were transiently transfected with either wild-type or mutant forms of CSPα (Figures 5B and C). Co-expression of eGFP was used as a marker of transiently transfected CAD cells. The elevated cellular expression of BK channels in the presence of dysfunctional CSPα mutants shown in Figure 5B thus mimics the functional increase in BK current density, as determined by single cell patch clamp recordings (Figure 3A). Whereas transient expression of wild-type CSPα did not significantly alter BK current density, it did reduce BKα subunit staining in BK stable CAD cells (Figure 5B). This difference likely reflects the ability of immunocytochemistry to detect intracellular and cell surface pools of BK channels, the former of which may be more readily affected by increased levels of wild-type CSPα. Note that only very low background fluorescence was detected in BK stable CAD cells stained with only fluorescently-labeled secondary antibody (Figure 5B, 2° Ab alone).

Discussion

This study identifies the co-chaperone CSPα (DnaJC5) as a critical regulator of BK channel density in the neuronal plasma membrane. In CSPα null mice, we observed a ~2.5-fold increase in the level of BK channel protein in CNS synaptosomal fractions compared with wild-type littermates (Figure 1); interestingly, the levels of other neuronal channels (i.e. $Ca_v2.2$, $K_v1.1$ and $K_v1.2$) were unchanged by KO of CSPα. Consistent with this novel finding in mice, we further observed that BK channel levels were dramatically increased in murine CNS-derived neuroblastoma cells following expression of a dominant negative form of CSPα containing a mutated HPD sequence (Figures 2 and 3). The HPD motif is essential for the overall activity of the heterotrimeric CSPα chaperone complex. Collectively these fundamental observations imply that CSPα normally acts to dampen or limit BK channel density at the cell surface, and that silencing or disruption of CSPα's activity leads to increased channel expression.

Biologically, it is possible that wild type CSPα limits BK channels by a cellular control mechanism in which CSPα acts to (1) reduce export of BK channels from the endoplasmic reticulum to the cell membrane and/or (2) increase channel removal/exit from the plasma membrane

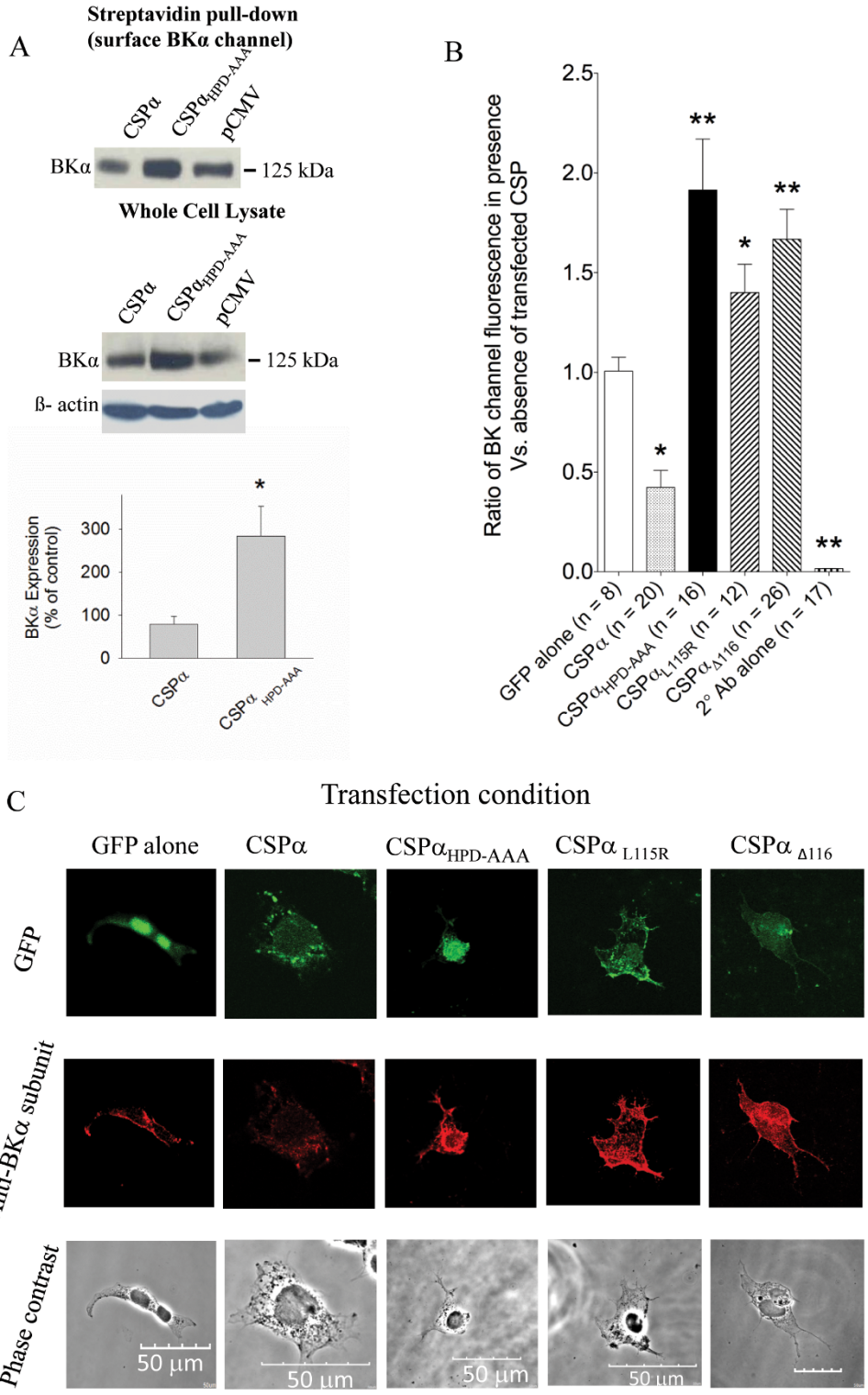

Figure 5 | CSPα$_{HPD-AAA}$ increases cell surface expression of BK channel stably-transfected CAD cells. (A) CAD cells stably-expressing BK channels were transiently-transfected with 0.75 µg CSPα, CSPα$_{HPD-AAA}$ and pCMV (negative control). 48 h post-transfection, the cells were labeled for 30 min at 4°C with bath applied Biotin. Following lysis, 1 mg of soluble protein lysate was subjected to overnight streptavidin pull-down at 4°C. Proteins isolated by streptavidin pull down (panel A, left) and 30 µg of soluble cellular lysate (panel A, right) were analyzed by Western Blot with an anti-BKα subunit antibody. β-actin (lower) is shown as a sample loading control. The BKα subunit data shown in the upper image of panel A were selected from a full-length western blot, which is displayed in Supplementary Figure 2B. The histogram in (panel B) quantifies the relative changes in cellular BK channel expression in the presence of WT and various mutant forms of CSPα (i.e. HPD-AAA, CSPα$_{L115R}$ and CSPα$_{Δ116}$), as depicted in panel C. Data are presented as mean ± SE; the number of cells analyzed under each condition is indicated in parentheses. Statistically significant differences were determined using a one-way ANOVA and a Dunnett post-hoc test (vs. GFP alone); * ($p<0.05$), ** ($p<0.01$). (C) Immunocytochemistry of BK stable CAD cells transiently transfected with GFP and various forms of CSPα. Transfected CAD cells were immunostained with an anti-BKα subunit antibody and examined by fluorescence microscopy (see Methods). Quantified fluorescence signal intensities for BKα subunit expression (as shown in red) under all treatments were normalized to the GFP alone condition. Displayed data are representative of three separate experiments.

to lysosomes or proteasomes. Inactivation of CSPα, either by mutations or loss of the protein, disrupts this regulatory activity, thereby allowing BK channels to accumulate at the cell surface. Such regulatory steps are not without precedent; earlier studies demonstrate that CSPα and Hsp40 limit the exit of the cystic fibrosis transmembrane conductance regulator (CFTR channel) from the ER[39,56], while DnaJA1 and DnaJA2 similarly reduce ER export of the hERG (human ether-a-go-go related gene) channel[37]. Our data showing that BK channels are also targeted by CSPα are consistent with this general paradigm. However, an alternate scenario whereby CSPα targets other cellular proteins (e.g. transport machinery) that in turn regulate BK export to/retrieval from the plasma membrane is also possible. Fernandez-Chacon's group has found a defect in synaptic vesicle recycling at motor nerve terminals in CSPα null mice[32] and Chandra's group has found that CSPα regulates polymerization of dynamin, an essential component of the endocytotic machinery[24], pointing to synaptic vesicle trafficking issues. The defective assembly of the exocytotic machinery due to reduced SNAP25 levels reported by Sudhof and colleagues makes a further case for changes in neuronal membrane trafficking in the absence of CSPα[30,31]. The role that these other CSPα clients may play in BK channel proteostasis remains to be determined. That said, it is clear from the data presented in Figure 1 that the CSPα-related increase in neuronal BK channel expression is selective, based on the absence of change found in $Ca_v2.2$, $K_v1.1$ and $K_v1.2$ protein levels. In this way, the cellular chaperone system, in addition to making 'decisions' about the folding/misfolding status of cellular ion channels, also monitors BK channel density. An interesting extension of the present study will be to investigate the role that CSPα plays in modulating mutant BK channels (e.g. D434G) associated with human epilepsy and movement disorders[11].

Our data further indicate that the recently identified, human disease-associated CSPα mutations $CSP\alpha_{\Delta 116}$ and $CSP\alpha_{L115R}$ are also capable of increasing BK current, suggesting that the neuronal sorting and trafficking of BK channels is altered by these mutations within the cysteine string region. While $CSP\alpha_{\Delta 116}$ and $CSP\alpha_{L115R}$ increase BK channel density at the membrane, the increase is not as large as that observed with $CSP\alpha_{HPD\text{-}AAA}$ (Figure 3), suggesting that $CSP\alpha_{\Delta 116}$ and $CSP\alpha_{L115R}$ mutations may result in only a partial loss of CSPα function. These same mutations were recently identified as the cause of ANCL in young adults[52–54] and lead to lysosomal accumulation of lipofuscin, along with dementia and motor deficits. Current understanding of CSPα's link to lysosomal dysfunction, ceroid deposition and synapse maintenance is limited.

Is CSPα dysfunction involved in diseases other than ANCL? Although dysfunction of CSPα, through either mutations or genetic deletion, has been linked to synaptic loss, the involvement of CSPα in neurodegenerative diseases other than ANCL is not clear. CSPα is reduced in the frontal cortex of humans with Alzheimer's disease[24] suggesting that a reduction in CSPα's neuroprotective capacity plays a role in Alzheimer's disease progression. Rescue of CSPα null mice with α-synuclein, but not α-synuclein A30P, the mutation associated with Parkinson's disease, implies a link between CSPα and the degenerative cascade in Parkinson's disease[29]. In experimental models, mutant huntingtin interferes with CSPα chaperone activity, suggesting that CSPα is compromised in Huntington's disease[57]. It is also reported that CSPα is reduced in rats following chronic morphine administration[58,59]. Despite these reported connections between reduced CSPα activity and the pathogenesis underlying distinct neurodegenerative diseases, numerous details remain to be established regarding the potential causality between CSPα dysfunction and the loss of synaptic integrity. Growing evidence suggests that the large J protein family, acting in concert with Hsc70/Hsp70, has links to neural diseases. In addition to the mutations in DnaJC5 (CSPα) associated with ANCL, mutations in the related J protein DnaJC6 (auxilin) results in juvenile Parkinsonism[59]. Similarly, mutations in sacin lead to autosomal recessive spastic ataxia of Charlevoix-Saguenay[60], mutations in DnaJB2 (HSJ1) cause lower motor neuron disease[61], while mutations in DnaJB6 (mrj) are implicated in muscular dystrophy[62], Parkinson's[63] and Huntington's disease[64].

Does BK channel over-expression contribute to degeneration under conditions in which CSPα is absent or dysfunctional? CSPα-mediated changes in BK levels may potentially contribute to the progressive activity-dependent neurodegeneration associated with CSPα loss/dysfunction, however there is currently no direct evidence supporting this idea. Indeed, high levels of BK channels in nerve terminals would be predicted to alter membrane excitability and could explain the increased synaptic depression in CSPα null mice observed by Sudhof and colleagues[14]. The severe age-dependent[14] and activity-dependent degeneration[22,23] of synaptic function in CSPα KO mice argue that increased BK channel activity may be intimately involved in the pathogenic sequence of events that lead to synaptic deterioration; however this scenario has not been directly examined thus far. Future studies will undoubtedly explore the potential link between BK channel-associated neuropathies (i.e. ataxia, epilepsy) and CNS vulnerability to neurodegeneration in the absence of CSPα.

In summary, our data demonstrate that CSPα is capable of regulating BK channel expression in a neuronal cell model and establish key residues within CSPα for this regulatory activity. Mutations of CSPα in the N terminal J domain or central cysteine string region lead to an increase in total and cell surface BK channel expression, resulting in greater BK channel current density. In parallel, increased BK channel expression is also found in the brain of CSPα null mouse, demonstrating that loss of CSPα function alters BK channel expression in the intact CNS, which may lead to altered neuronal membrane excitability (Figure 6). Based on these findings, we speculate that alterations in the cell surface expression of neuronal BK channels may contribute to the pathogenesis of neurodegeneration associated with either genetic loss or dysfunction of CSPα.

Methods

Cell culture. CAD (CNS catecholaminergic derived) mouse neuroblastoma cells were seeded into 6 well plates and grown in DMEM/F12 medium supplemented with 10% fetal bovine serum and 1% penicillin/streptomycin, as previously described[42,65]. The established rat aortic smooth muscle cell line A7r5 was grown in DMEM containing 10% FBS, as described previously[55]. Cells were lysed in 40 mM Tris (pH 7.4), 150 mM NaCl, 2 mM EDTA, 1 mM EGTA, 1 mM Na_3VO_4, 0.1% SDS, 1% (v/v) Triton X-100, 0.5 mM PMSF and protease inhibitor (Sigma) at 4°C for 1 hour. Lysates were centrifuged at 15000 × g for 5 minutes at 4°C and the supernatant (soluble fraction) was collected and stored at −70°C. For transient transfection, CAD cells grown on 35 mm dishes were washed in PBS and transiently transfected using ~1.5 μg of cDNA and 7 μl of Lipofectamine-2000 (Invitrogen) per dish. Reagents were mixed in 0.2 ml of Opti-MEM medium and then diluted to a total volume of 1 ml with DMEM. Protein concentration of the soluble CAD cell lysate was determined using the Bradford assay (BioRad).

Immunoblotting. Proteins were electrotransferred from polyacrylamide gels to nitrocellulose membrane (0.2 μm pore size) in 20 mM Tris, 150 mM glycine and 12% methanol. Membranes were blocked in phosphate-buffered saline (PBS) containing 0.1% Tween 20, 4% (w/v) skim milk powder and then incubated with primary antibody overnight at 4°C. The membranes were washed and incubated with horseradish peroxidase-coupled secondary antibody for ~2 h at room temperature. Bound antibodies on the membranes were detected by incubation with the West Pico chemiluminescence reagent (Pierce Chemical Co.) and exposure to Kodak x-ray film. The chemiluminscent signals were quantified using a Biorad Fluor-S MultiImager Max and Quantity One 4.2.1 software. Representative western blot data were gathered from single blots and single exposures. Primary antibodies were obtained as follows: BK polyclonal and $Ca_v2.2$ polyclonal (Millipore), BK monoclonal, c-myc monoclonal and flotillin monoclonal (BD Biosciences), $K_v1.1$ monoclonal and $K_v1.2$ monoclonal (NeuroMab), SNAP25 monoclonal (Sternberger monoclonals), syntaxin monoclonal, GAP43 monoclonal, and β-actin monoclonal (Sigma-Aldrich).

Quantitative Real Time-PCR. Whole brains were dissected from CSPα null and wild-type mice and immediately frozen at −80°C. Total RNA was isolated using the RNeasy Lipid Tissue Mini Kit (Qiagen) and reverse transcription was performed with 1 μg total RNA using the Quantitect Reverse Transcription Kit (Qiagen) following the manufacturer's instructions. For the negative control groups, all components except the reverse transcriptase were included in the reaction mixtures. Real-Time

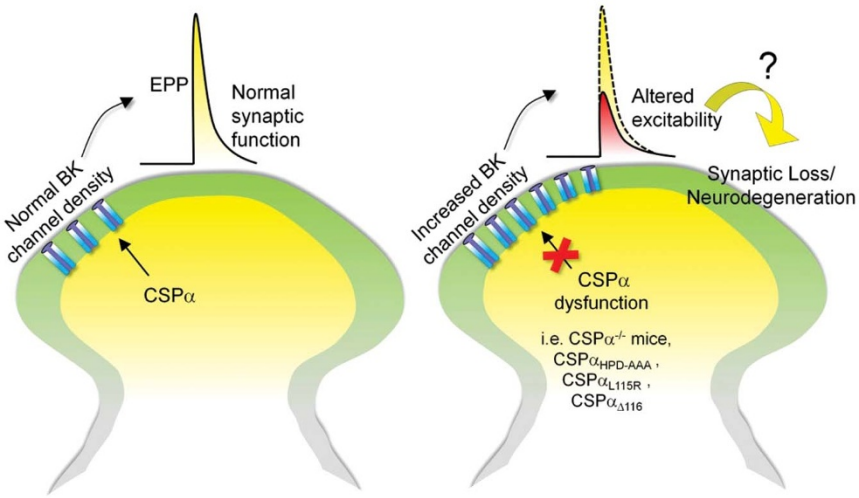

Figure 6 | Cartoon highlighting the impact of CSPα dysfunction on BK channel density in the synaptic membrane and possible resulting changes in membrane excitability that may ultimately promote neurodegeneration.

PCR with either BKα subunit (KCNMA1) primers (Forward: 5′-TCTCAGCATTG GTGCCCTCGTAAT-3′ Reverse: 5′-GTAGAGGAGGAAGAACACGTTGAA-3′) or actin (ACTB) primers (Forward: 5′ ACTGTCGAGTCGCGTCCA-3′ Reverse: 5′ GCAGCGATATCGTCATCCAT-3′) was performed using the Quantitect SYBR green PCR kit (Qiagen). Mouse ACTB was utilized as the reference gene. The running protocol involved 40 cycles consisting of sequential incubations at 94°C for 15 s, 55°C for 30 s and 72°C for 15 s using an Eppendorf Realplex 4 Mastercycler. PCR specificity was confirmed by dissociation curve analysis. Quantification cycle values (C_q) were determined with Realplex version 1.5 software, using the software's default noise band settings to determine the threshold fluorescence. Relative expression of KCNMA1 normalized to the ACTB reference gene in CSPα KO versus wild-type mice was determined using the $2^{-\Delta\Delta C_q}$ method (Table 1).

PCR assay validation was performed by testing serial dilutions of pooled template cDNAs, which indicated a linear dynamic range of 33–0.0033 ng template and yielded standard curves with slopes of −3.53 and −3.31 for KCNMA1 and ACTB, respectively, and R^2 values >0.99 and percent efficiencies of 91.8 and 100.3% for KCNMA1 and ACTB, respectively. No fluorescence was detected in negative template controls. RNA integrity was confirmed by performing agarose gel electrophoresis of the isolated mouse brain total RNA preparations denatured with glyoxal sample buffer (Ambion). This analysis yielded intensity ratios between the 28 S and 18 S rRNA bands of 1.85–2.04 for all the samples tested[66].

Biotinylation of cell surface BK channels. CAD cells stably expressing murine brain BKα subunits[43] were transfected with CSPα variants, as described above. 24 h post-transfection, the cells were washed three times with PBS. CAD cells were then incubated with EZ-Link Sulfo-NHS-SS Biotin (Thermo Scientific) (1 μg/ml) in PBS for 30 min at 4°C. As a negative control, cells were incubated only with PBS. The reaction was neutralized by addition of 1% (w/v) BSA in PBS for 10 min at 4°C. After neutralization, cells were washed thrice with ice-cold PBS to remove non-reacted biotin, and were harvested in 1 ml of PBS containing 1% v/v Triton X-100 and protease inhibitor (complete, EDTA-free, Sigma) by an incubation for 2–5 minutes on ice. The lysates were centrifuged at 15,000 × g for 15 min at 4°C and the soluble protein concentration was determined using the Bradford assay (Bio Rad).

For streptavidin pull-down, 1 mg of the soluble protein lysate was incubated with 100 μl streptavidin agarose beads (50% slurry) (Thermo Scientific) overnight at 4°C on a rotator. Beads were rinsed thrice with 1% Triton X-100 in PBS. Biotinylated proteins were eluted from the beads by adding 2× Laemmli sample buffer (62.2 mM Tris HCl pH 6.8, 7.5% v/v Glycerol, 2% w/v SDS, 0.015 mM Bromophenol Blue, 1.2% v/v β-Mercaptoethanol and 100 mM DTT) and treating the samples at 37°C for 1 h. Following elution, proteins were separated by SDS-PAGE using a 10% polyacrylamide gel and BKα subunits were detected by Western blot analysis.

Stable transfection of CAD cells. To establish a stable BK channel expressing cell line, CAD cells were transiently transfected in 100 mm culture plates with pcDNA3.1 Zeo(+) plasmid containing cDNA encoding a BKα subunit originally cloned from murine brain[43]. 48 h post-transfection, cells were plated and grown in media containing 0.8 mg/ml Zeocin (Invitrogen). Non-transfected cells were used as negative control. The selection medium was switched every 3 to 4 days until cell foci were identified. Cell foci were isolated with cloning cylinders and transferred into 12-well plates before expanding colonies in 6-well plates. The stable expression of the BK channel was confirmed by Western blot analysis and immunocytochemistry. Individual CAD cell clones stably expressing BKα subunits were subsequently maintained in DMEM/F12 medium containing 0.5 mg/ml Zeocin.

Whole cell patch clamp recordings. Voltage-clamp measurements were performed using conventional, ruptured membrane patch clamp methodology in combination with an Axopatch 200B amplifier, Digidata 1440 series analogue/digital interface and pClamp v10 software. Whole cell electrical signals were typically filtered at 1–2 kHz and sampled at 5 kHz. Glass micropipettes (2–4 MΩ tip resistance) were pulled from thin-walled borosilicate capillaries and contained 100 mM KOH, 30 mM KCl, 1 mM $MgCl_2$, 0.005 mM $CaCl_2$, 10 mM HEPES, pH 7.3 with methanesulfonic acid. The bath chamber was placed on the stage of Nikon TE2000 inverted microscope equipped with epifluorescence illumination and perfused with a modified Ringer's saline solution containing 135 mM NaCl, 5 mM KCl, 1 mM $MgCl_2$, 2.5 mM $CaCl_2$, 5 mM 4-aminopyridine and 10 mM HEPES, pH 7.3 with 1N NaOH. Cells in the bath chamber were constantly superfused at ~2 ml/min and solution changes were performed by gravity flow from a series of elevated solution reservoirs using manually controlled solenoid valves. All electrophysiological recordings were performed at 35–37°C. CAD cells stably expressing BK channels were transiently transfected with either wild-type or mutant CSPα cDNA constructs, together with eGFP. Transfected cells were identified in the recording bath by their green fluorescence using 488 nm excitation and 510 nm emission filters.

Immunocytochemistry. Transfected CAD cells were plated on sterile glass coverslips and washed three times with PBS to remove medium and serum, then fixed by incubation for 25 min at room temperature in PBS containing 1% (w/v) formalin. Cells were washed thrice with PBS and permeabilized by incubation for 5 min in PBS containing 0.01% Triton X-100. Cells were then washed three times in PBS and incubated in blocking solution (5% v/v donkey serum, 0.05% v/v Tween-20 in PBS) to reduce non-specific antibody binding. Cells were then incubated with anti-BK channel polyclonal antibody (Millipore, 1 : 400 dilution) overnight at 4°C in blocking solution, then washed five times with PBS. Cells were incubated at 4°C for 1 hour in blocking solution containing goat anti-rabbit secondary antibody conjugated to Cy3 (Jackson ImmunoResearch, 1 : 2000). Cells were rinsed once with blocking solution and washed three times with PBS. Coverslips containing stained cells were mounted onto glass slides with a drop of mounting media (Prolong Gold, anti-fade, Invitrogen) and images were taken on an Olympus Fluoview FV10i confocal microscope using a 60× (oil immersion) objective (NA:1.35). Laser intensity and sensitivity were maintained at 40% for all images, with a confocal aperture of 1.35. Fluorescence signal intensities of individual cells were analyzed and quantified using CellSens Dimension digital imaging software (Olympus).

Isolation of Tissue Fractions from Mouse Brain and Aorta. CSPα$^{-/+}$ mice were obtained from Jackson Labs (Bar Harbor, Maine) and genotyped as previously described[14]. All mice were maintained in accordance with an animal protocol approved by the University of Calgary and the Guidelines for Lab Animal Safety (NIH). Mice (age 23–27 days) were anesthetized with isofluorane and euthanized and intact brain tissue obtained from wild-type, heterozygote and CSPα KO mice were fractionated. Briefly, a mouse brain was homogenized in 7 mls of ice cold 0.32 M sucrose, 10 mM HEPES, 1 mM EGTA, 0.1 mM EDTA and 0.3 mM PMSF with 15 up and down strokes using a Teflon glass homogenizer. The homogenate was centrifuged at 4°C for 7 min at 1,000 × g and the supernatant (S1) collected. The S1 supernatant was then spun for 15 min at 22,000 × g and the resulting supernatant (S2) was discarded. The pellet (P2) was washed by re-suspension in the above sucrose solution and then re-centrifuged at 22,000 × g. The final pellet, representing washed-crude synaptosomes, was re-suspended in 4 ml of sucrose buffer.

Thoracic and abdominal aorta was removed following euthanasia and cleaned of extraneous tissue. Each isolated aorta was then placed in an Eppendorf tube,

immediately frozen on dry ice and stored at −80°C. Thawed aortic tissue was minced into small pieces and then disrupted in the tube using a tight-fitting plastic pestle. Tissue pieces were suspended in 0.2–0.3 ml of ice-cold solubilization buffer (10 mM Tris HCl pH 7.5, 150 mM NaCl, 1% Triton X-100, 1 mM EDTA, 1 mM EGTA, 1 mM benzamidine, and 5 μg/ml each of leupeptin, aprotinin and pepstatin A) and kept on ice for 45–60 min with occasional mixing. The crude homogenate was then centrifuged at 1000 × g for 5 min at 4°C and the supernatant was collected. Following determination of protein concentration, the soluble fraction was used for Western blot analysis.

1. Gu, N., Vervaeke, K. & Storm, J. F. BK potassium channels facilitate high-frequency firing and cause early spike frequency adaptation in rat CA1 hippocampal pyramidal cells. *J Physiol* **580**, 859–882 (2007).
2. Haghdoost-Yazdi, H., Janahmadi, M. & Behzadi, G. Iberiotoxin-sensitive large conductance Ca2+ -dependent K+ (BK) channels regulate the spike configuration in the burst firing of cerebellar Purkinje neurons. *Brain Res* **1212**, 1–8 (2008).
3. Faber, E. S. & Sah, P. Calcium-activated potassium channels: multiple contributions to neuronal function. *Neuroscientist.* **9**, 181–194 (2003).
4. Roberts, W. M., Jacobs, R. A. & Hudspeth, A. J. Colocalization of ion channels involved in frequency selectivity and synaptic transmission at presynaptic active zones of hair cells. *J Neurosci* **10**, 3664–3684 (1990).
5. Robitaille, R., Garcia, M. L., Kaczorowski, G. J. & Charlton, M. P. Functional colocalization of calcium and calcium-gated potassium channels in control of transmitter release. *Neuron* **11**, 645–655 (1993).
6. Raffaelli, G., Saviane, C., Mohajerani, M. H., Pedarzani, P. & Cherubini, E. BK potassium channels control transmitter release at CA3-CA3 synapses in the rat hippocampus. *J Physiol* **557**, 147–157 (2004).
7. Hu, H. *et al.* Presynaptic Ca2+-activated K+ channels in glutamatergic hippocampal terminals and their role in spike repolarization and regulation of transmitter release. *J Neurosci* **21**, 9585–9597 (2001).
8. Martire, M. *et al.* Pre-synaptic BK channels selectively control glutamate versus GABA release from cortical and hippocampal nerve terminals. *J Neurochem* **115**, 411–422 (2010).
9. Brenner, R. *et al.* BK channel beta4 subunit reduces dentate gyrus excitability and protects against temporal lobe seizures. *Nat Neurosci* **8**, 1752–1759 (2005).
10. Sausbier, M. *et al.* Cerebellar ataxia and Purkinje cell dysfunction caused by Ca2+-activated K+ channel deficiency. *Proc Natl Acad Sci U S A* **101**, 9474–9478 (2004).
11. Du, W. *et al.* Calcium-sensitive potassium channelopathy in human epilepsy and paroxysmal movement disorder. *Nat Genet* **37**, 733–738 (2005).
12. Diez-Sampedro, A., Silverman, W. R., Bautista, J. F. & Richerson, G. B. Mechanism of increased open probability by a mutation of the BK channel. *J Neurophysiol.* **96**, 1507–1516 (2006).
13. Zinsmaier, K. E., Eberle, K. K., Buchner, E., Walter, N. & Benzer, S. Paralysis and early death in cysteine string protein mutants of Drosophila. *Science* **263**, 977–980 (1994).
14. Fernandez-Chacon, R. *et al.* The synaptic vesicle protein CSP alpha prevents presynaptic degeneration. *Neuron* **42**, 237–251 (2004).
15. Zhao, X., Braun, A. P. & Braun, J. E. Biological Roles of Neural J Proteins. *Cell Mol. Life Sci* **65**, 2385–2396 (2008).
16. Braun, J. E. & Scheller, R. H. Cysteine string protein, a DnaJ family member, is present on diverse secretory vesicles. *Neuropharmacology* **34**, 1361–1369 (1995).
17. Greaves, J. & Chamberlain, L. H. Dual Role of the Cysteine-String Domain in Membrane Binding and Palmitoylation-dependent Sorting of the Molecular Chaperone Cysteine-String Protein. *Mol. Biol Cell* **11**, 4748–4759 (2006).
18. Ohyama, T. *et al.* Huntingtin-interacting protein 14, a palmitoyl transferase required for exocytosis and targeting of CSP to synaptic vesicles. *J Cell Biol* **179**, 1481–1496 (2007).
19. Braun, J. E., Wilbanks, S. M. & Scheller, R. H. The cysteine string secretory vesicle protein activates Hsc70 ATPase. *J Biol Chem* **271**, 25989–25993 (1996).
20. Stahl, B., Tobaben, S. & Sudhof, T. C. Two distinct domains in hsc70 are essential for the interaction with the synaptic vesicle cysteine string protein. *Eur J Cell Biol* **78**, 375–381 (1999).
21. Chamberlain, L. H. & Burgoyne, R. D. Activation of the ATPase activity of heat-shock proteins Hsc70/Hsp70 by cysteine-string protein. *Biochem J* **322(Pt 3)**, 853–858 (1997).
22. Schmitz, F. *et al.* CSPalpha-deficiency causes massive and rapid photoreceptor degeneration. *Proc Natl Acad Sci U S A* **103**, 2926–2931 (2006).
23. Garcia-Junco-Clemente, P. *et al.* Cysteine string protein-alpha prevents activity-dependent degeneration in GABAergic synapses. *J Neurosci* **30**, 7377–7391 (2010).
24. Zhang, Y. Q. *et al.* Identification of CSPalpha Clients Reveals a Role in Dynamin 1 Regulation. *Neuron* **74**, 136–150 (2012).
25. Magga, J. M., Jarvis, S. E., Arnot, M. I., Zamponi, G. W. & Braun, J. E. Cysteine string protein regulates G-protein modulation of N-type calcium channels. *Neuron* **28**, 195–204 (2000).
26. Jarvis, S. E., Magga, J. M., Beedle, A. M., Braun, J. E. & Zamponi, G. W. G protein modulation of N type calcium channels is facilitated by physical interactions between syntaxin 1A and Gbetagamma. *J Biol Chem* **275**, 6388–6394 (2000).
27. Leveque, C. *et al.* Interaction of cysteine string proteins with the alpha1A subunit of the P/Q-type calcium channel. *Journal of Biological Chemistry* **273**, 13488–13492 (1998).
28. Gundersen, C. B. & Umbach, J. A. Suppression cloning of the cDNA for a candidate subunit of a presynaptic calcium channel. *Neuron* **9**, 527–537 (1992).
29. Chandra, S., Gallardo, G., Fernandez-Chacon, R., Schluter, O. M. & Sudhof, T. C. Alpha-synuclein cooperates with CSPalpha in preventing neurodegeneration. *Cell* **123**, 383–396 (2005).
30. Sharma, M., Burre, J. & Sudhof, T. C. CSPalpha promotes SNARE-complex assembly by chaperoning SNAP-25 during synaptic activity. *Nat Cell Biol* **13**, 30–39 (2011).
31. Sharma, M. *et al.* CSPalpha knockout causes neurodegeneration by impairing SNAP-25 function. *EMBO J* **31(4)**: 829–41 (2011).
32. Rozas, J. L. *et al.* Motorneurons Require Cysteine String Protein-alpha to Maintain the Readily Releasable Vesicular Pool and Synaptic Vesicle Recycling. *Neuron* **74**, 151–165 (2012).
33. Shruti, S. *et al.* The brain-specific Beta4 subunit downregulates BK channel cell surface expression. *PLoS. ONE.* **7**, e33429 (2012).
34. Schubert, R. & Nelson, M. T. Protein kinases: tuners of the BKCa channel in smooth muscle. *Trends Pharmacol. Sci.* **22**, 505–512 (2001).
35. Shipston, M. J. Ion channel regulation by protein palmitoylation. *J. Biol. Chem.* **286**, 8709–8716 (2011).
36. Shipston, M. J. Alternative splicing of potassium channels: a dynamic switch of cellular excitability. *Trends Cell Biol.* **11**, 353–358 (2001).
37. Walker, V. E. *et al.* Hsp40 chaperones promote degradation of the HERG potassium channel. *J Biol Chem* **285**, 3319–3329 (2010).
38. Baaklini, I. *et al.* The DNAJA2 substrate release mechanism is essential for chaperone-mediated folding. *J. Biol. Chem.* **287(50)**: 41939–54 (2012).
39. Schmidt, B. Z., Watts, R. J., Aridor, M. & Frizzell, R. A. Cysteine string protein promotes proteasomal degradation of the cystic fibrosis transmembrane conductance regulator (CFTR) by increasing its interaction with the C terminus of Hsp70-interacting protein and promoting CFTR ubiquitylation. *J Biol Chem* **284**, 4168–4178 (2009).
40. Yan, F. F. *et al.* Role of Hsp90 in biogenesis of the beta-cell ATP-sensitive potassium channel complex. *Mol. Biol Cell* **21**, 1945–1954 (2010).
41. Brown, H. *et al.* Cysteine string protein (CSP) is an insulin secretory granule-associated protein regulating beta-cell exocytosis. *EMBO J* **17**, 5048–5058 (1998).
42. Xu, F. *et al.* Quercetin targets cysteine string protein (CSPalpha) and impairs synaptic transmission. *PLoS. ONE.* **5**, e11045 (2010).
43. Butler, A., Tsunoda, S., McCobb, D. P., Wei, A. & Salkoff, L. mSlo, a complex mouse gene encoding "maxi" calcium-activated potassium channels. *Science* **261**, 221–224 (1993).
44. Kampinga, H. H. & Craig, E. A. The HSP70 chaperone machinery: J proteins as drivers of functional specificity. *Nat Rev Mol. Cell Biol* **11**, 579–592 (2010).
45. Gibbs, S. J. *et al.* Hsp40 couples with the CSPalpha chaperone complex upon induction of the heat shock response. *PLoS. ONE.* **4**, e4595 (2009).
46. Swayne, L. A., Blattler, C., Kay, J. G. & Braun, J. E. A. Oligomerization charateristics of cysteine string protein. *Biochemical and Biophysical Research Communications* **300**, 921–926 (2003).
47. Brown, I. R. Heat shock proteins and protection of the nervous system. *Ann. N. Y. Acad Sci* (2007).
48. Fukata, Y. & Fukata, M. Protein palmitoylation in neuronal development and synaptic plasticity. *Nat. Rev. Neurosci.* **11**, 161–175 (2010).
49. Kang, R. *et al.* Neural palmitoyl-proteomics reveals dynamic synaptic palmitoylation. *Nature* **456**, 904–909 (2008).
50. Betz, A. *et al.* Munc13-1 is a presynaptic phorbol ester receptor that enhances neurotransmitter release. *Neuron* **21**, 123–136 (1998).
51. Knaus, H. G. *et al.* Tremorgenic indole alkaloids potently inhibit smooth muscle high-conductance calcium-activated potassium channels. *Biochemistry* **33**, 5819–5828 (1994).
52. Velinov, M. *et al.* Mutations in the Gene DNAJC5 Cause Autosomal Dominant Kufs Disease in a Proportion of Cases: Study of the Parry Family and 8 Other Families. *PLoS. ONE.* **7**, e29729 (2012).
53. Noskova, L. *et al.* Mutations in DNAJC5, encoding cysteine-string protein alpha, cause autosomal-dominant adult-onset neuronal ceroid lipofuscinosis. *Am. J Hum. Genet* **89**, 241–252 (2011).
54. Benitez, B. A. *et al.* Exome-sequencing confirms DNAJC5 mutations as cause of adult neuronal ceroid-lipofuscinosis. *PLoS. ONE.* **6**, e26741 (2011).
55. Kyle, B. D., Hurst, S., Swayze, R. D., Sheng, J. & Braun, A. P. Specific phosphorylation sites underlie the stimulation of a large conductance, Ca(2+)-activated K(+) channel by cGMP-dependent protein kinase. *FASEB J.* **27**, 2027–2038 (2013).
56. Zhang, H. *et al.* Cysteine string protein monitors late steps in cystic fibrosis transmembrane conductance regulator biogenesis. *J Biol Chem* **281**, 11312–11321 (2006).
57. Miller, L. C. *et al.* Cysteine String Protein (CSP) inhibition of N-type calcium channels is blocked by mutant huntingtin. *J Biol Chem* **278**, 53072–53081 (2003).
58. Abul-Husn, N. S. *et al.* Chronic morphine alters the presynaptic protein profile: identification of novel molecular targets using proteomics and network analysis. *PLoS. ONE.* **6**, e25535 (2011).

59. Edvardson, S. *et al.* A Deleterious Mutation in DNAJC6 Encoding the Neuronal-Specific Clathrin-Uncoating Co-Chaperone Auxilin, Is Associated with Juvenile Parkinsonism. *PLoS. ONE.* **7**, e36458 (2012).
60. Girard, M. *et al.* Mitochondrial dysfunction and Purkinje cell loss in autosomal recessive spastic ataxia of Charlevoix-Saguenay (ARSACS). *Proc. Natl. Acad. Sci. U. S. A* **109**, 1661–1666 (2012).
61. Blumen, S. C. *et al.* A rare recessive distal hereditary motor neuropathy with HSJ1 chaperone mutation. *Ann. Neurol* **71**, 509–519 (2012).
62. Sarparanta, J. *et al.* Mutations affecting the cytoplasmic functions of the co-chaperone DNAJB6 cause limb-girdle muscular dystrophy. *Nat. Genet.* **44**, 450–452 (2012).
63. Durrenberger, P. F. *et al.* DnaJB6 is present in the core of Lewy bodies and is highly up-regulated in parkinsonian astrocytes. *J. Neurosci. Res.* **87**, 238–245 (2009).
64. Chuang, J. Z. *et al.* Characterization of a brain-enriched chaperone, MRJ, that inhibits huntingtin aggregation and toxicity independently. *J Biol Chem* **277**, 19831–19838 (2002).
65. Rosales-Hernandez, A., Beck, K. E., Zhao, X., Braun, A. P. & Braun, J. E. RDJ2 (DNAJA2) chaperones neural G protein signaling pathways. *Cell Stress. Chaperones.* **14**, 71–82 (2008).
66. Bustin, S. A. *et al.* The MIQE guidelines: minimum information for publication of quantitative real-time PCR experiments. *Clin. Chem.* **55**, 611–622 (2009).

Author contributions

B.D.K. and E.A. performed the experiments and prepared the figures and are equal contributors. We thank Dr. Frank Visser and Ms. Mary Resek and Mr. Sam Braun for excellent technical support. J.E.A.B. and A.P.B. designed the study and wrote the manuscript. All authors contributed to the writing and revision of the manuscript.

Additional information

Supplementary information accompanies this paper at http://www.nature.com/scientificreports

Competing financial interests: The authors declare no competing financial interests.

How to cite this article: Kyle, B.D., Ahrendt, E., Braun, A.P. & Braun, J.E.A. The Large Conductance, Calcium-activated K^+ (BK) Channel is regulated by Cysteine String Protein. *Sci. Rep.* **3**, 2447; DOI:10.1038/srep02447 (2013).